Brazilian Journal of Biology®

ISSN 1519-6984 (Print)
ISSN 1678-4375 (Online)

Original Article

Molecular docking, ADMET and molecular dynamics simulation revealed metralindole as a multitargeted inhibitor for division kinases

Ancoragem molecular, ADMET e simulação de dinâmica molecular revelaram o metralindol como inibidor multialvo para divisão quinases

I. Al-Dhuayan[a*] and N. K. ALaqeel[a*]

[a]Imam Abdulrahman Bin Faisal University, College of Science, Department of Biology, Dammam, Saudi Arabia

Abstract

Lung cancer is the most common type of cancer in the world, and alone, in 2020, almost 2.21 million new cases were diagnosed, with 1.80 million deaths, and are increasing daily. Non-small cell lung (NSCLC) is the primary type of lung cancer, predominantly forms around 80% of cases compared to small cell carcinoma, and about 75% of patients are already in an advanced state when diagnosed. Despite notable advances in early diagnosis and treatment, the five-year survival rate for NSCLC is not encouraging. Therefore, it is crucial to investigate the molecular causes of non-small cell lung cancer to create more efficient therapeutic approaches. Lung cancer showed a more significant and persistent binding affinity and energy landscape with the target CDK2 staurosporine and FGF receptor-1. In this study, we have picked two essential target proteins, human cyclin-dependent kinase-2 and Human Protein Kinase CK2 Holoenzyme and screened the entire prepared DrugBank prepared library of 1,55,888 compounds and identified 2-(2-methyl-5-nitroimidazole-1-yl) ethanol (Metralindole) as a major inhibitor. Metralindole has displayed high docking scores of -5.159 Kcal/mol and -5.99 Kcal/mol with good hydrogen bonding and other bonding topologies such as van der Waals force, and ADMET results shown excellent bioavailability, outstanding solubility, no side effects, and toxicity. The molecular dynamics simulation for 100ns in a water medium confirmed the compound's stability and interaction pattern with the lowest deviation and fluctuations. Our in-silico study suggests Metralindole, an experimental compound, can effectively cure lung cancer. Further, the experimental validation of the compound is a must before any prescription.

Keywords: lung cancer, metralindole, molecular docking, molecular dynamics simulation, kinase.

Resumo

O câncer de pulmão é o tipo de câncer mais comum no mundo, e, apenas em 2020, foram diagnosticados quase 2,21 milhões de novos casos, com 1,8 milhão de óbitos, e isso vem aumentando diariamente. O câncer de pulmão de células não pequenas (CPCNP) é o tipo primário de câncer de pulmão, forma que predomina em cerca de 80% dos casos em comparação com o carcinoma de pequenas células, e cerca de 75% dos pacientes já estão em estado avançado quando diagnosticados. Apesar dos avanços notáveis no diagnóstico e tratamento precoces, a taxa de sobrevida em cinco anos para CPCNP não é animadora. Portanto, é crucial investigar as causas moleculares do CPCNP para criar abordagens terapêuticas mais eficientes. O câncer de pulmão mostrou uma afinidade de ligação e perfil energético mais significativos e persistentes com a estaurosporina CDK2 alvo e o receptor-1 de FGF. Neste estudo, escolhemos duas proteínas-alvo essenciais, a quinase dependente de ciclina humana-2 e a holoenzima CK2 da proteína quinase humana, examinamos toda a biblioteca preparada pelo DrugBank de 1,55,888 compostos e identificamos 2-(2-metil-5-nitroimidazol-1-il) etanol (metralindol) como inibidor principal. O metralindol apresentou altas pontuações de ancoragem de -5,159 Kcal/mol e -5,99 Kcal/mol, com boas ligações de hidrogênio e outras topologias de ligação, como a força de Van der Waals, e os resultados do ADMET mostraram excelente biodisponibilidade e solubilidade, sem efeitos colaterais e toxicidade. A simulação de dinâmica molecular para 100ns em meio aquoso confirmou a estabilidade e o padrão de interação do composto com os menores desvios e flutuações. Nosso estudo in silico sugere que o metralindol, um composto experimental, pode efetivamente curar o câncer de pulmão. Além disso, a validação experimental do composto é obrigatória antes de qualquer prescrição.

Palavras-chave: câncer de pulmão, metralindol, ancoragem molecular, simulação de dinâmica molecular, quinase.

*e-mail: ialdhuayan@iau.edu.sa; nalaqeel@iau.edu.sa
Received: February 2, 2023 – Accepted: March 11, 2023

1. Introduction

One of the most prevalent malignant tumours in the world is lung cancer. The origin and course of lung cancer entail many coordinated phases, from DNA damage and mutations through field carcinogenesis and pre-neoplasia in the airway epithelium to the growth of the tumour (Nimsarkar et al., 2022; Fong et al., 1999). Oncogenes, tumour-suppressor genes (TSGs), and genes that promote genomic instability are among the genes that are most commonly mutated in cancer. When a single cellular lineage experiences several mutations, cancer develops. Cancer initiation takes place in the compartments that divide epithelial tissues. The cells in each compartment are constantly changing. A tiny number of stem cells divide and differentiate to replenish each compartment. Homeostatic mechanisms keep cell counts steady in healthy tissue. After treatment, cancer might occasionally return (Hou et al., 2022; Karwasra et al., 2022a, b; Khatami, 2017). It is known as a recurrence. Even if just one cancer cell is left, it can multiply and grow into a new tumour. Cancer may have travelled through the blood or lymphatic system to another part of the body where it has now developed into a new tumour, or it may have begun to grow in the same area of the body where it first appeared (Warburg, 1956; Zülch, 2013). Therefore, cancer that was receding or had vanished may now begin to grow and get larger. When the genes in cancer cells mutate, this may occur. Cancer cells can resist chemotherapy and other pharmacological therapies due to specific gene abnormalities (Ramlal et al., 2021; Tarique et al., 2021). Men have the highest lung cancer incidence rate, with women coming in second. A tumour is formed when specific lung cells turn aberrant and proliferate out of control (Alberg et al., 2007; Boyle and Maisonneuve, 1995). This condition is known as lung cancer. In its early stages, lung cancer may not show any signs or symptoms. Chest pain, frequent coughing, blood in the mucus, breathing difficulties, difficulty speaking or swallowing, loss of appetite and weight loss, exhaustion, or swelling in the face or neck are all symptoms of lung cancer. Other symptoms may appear if cancer spreads (metastasises) to other tissues. Also, there are many reports on machine learning and mobile application-based therapies that help to recover from disease and actively participate in the design development of drugs (Ahmad et al., 2021; Balasubramanian et al., 2021; Khan et al., 2021b; Tripathi et al., 2022; Yadav et al., 2022; Boice Júnior et al., 2022).

Adults in their sixties or seventies are the most likely to develop lung cancer. Although long-term tobacco use is a significant risk factor for lung cancer, the disease can also strike persons who have never smoked. Small cell carcinoma (SCLC) and non-small cell lung cancer (NSCLC) are the two kinds of lung cancer. About 85% of cases are NSCLC, and 75% of individuals with NSCLC were already in an advanced state when diagnosed (Chen et al., 2015). The overall survival rate for NSCLC remains low, and patients with advanced or metastatic disease have a worse prognosis, despite recent advancements in detection and therapy (Riudavets et al., 2022). The best treatments for advanced-stage NSCLC patients include chemotherapy and targeted biological therapy. Despite significant attempts to enhance treatment approaches over the past few decades, conventional therapies, including surgery, radiotherapy, and chemotherapy, still have poor clinical outcomes compared to other significant forms of cancer like colon, prostate, and breast cancers. Currently, FDA has approved various drug molecules, most of which are from a plant source and have been modified to get proper pocket coverage (Khuntia et al., 2022; Khan et al., 2021a; Kaul et al., 2020). The challenges in diagnosing lung cancer in its early stages and the high recurrence rate following curative treatments are the leading causes of the prognosis' lack of improvement. Biomedical researchers use proteomics, metabolomics, and lipidomics to study biomarkers further, or these disciplines may be combined. Various literatures suggested that multitargeted therapy can be a better option, but the side effects are yet to be evaluated for proper interpretations (Ahmad et al., 2022a, b, c; Alghamdi et al., 2022; Alturki et al., 2022; Alzamami et al., 2022; Zhang et al., 2017) .

In the present study, we have extensively analysed and reported the 2-(2-methyl-5-nitroimidazole-1-yl) ethanol (Metralindole) against lung cancer. This has been discovered through extensive computing with High Throughput Virtual Screening (HTVS), Standard Precision (SP), Extra Precise (XP), and Molecular Mechanics/Generalized Born Surface Area (MMGBSA) calculations to lower the computing costs with additional scoring. Additionally, we have extended the analysis with molecular dynamics (MD) simulations for 100ns for both protein-ligand complexes.

2. Materials and Methods

2.1. Protein preparation

We considered CK2 (Casein kinase II) with PDBID: 1JWH and CDK2 (Human Cyclin-Dependent Kinase 2) with PDBID: 1AQ1, which show primary indicators and play a role in the pathogenesis of lung cancer (Niefind et al., 2001; Lawrie et al., 1997). The CK2 protein is an enzyme that plays a crucial role in several cellular processes in humans. It regulates cell growth and division, DNA repair, transcription, translation, and signal transduction pathways. CK2 is a serine/threonine kinase, which means it adds phosphate groups to serine and threonine residues in target proteins, thereby regulating their activity. CDK2 is a serine/threonine kinase critical in regulating the cell cycle. CDK2 is a member of the CDK family of proteins, which are key cell division and proliferation regulators. CDK2 is activated by binding to cyclin E or cyclin A, which drives the progression of cells. The 3-D structure of both kinases was retrieved from the RCSB database to import the crystal structure into the Schrodinger Maestro workspace for protein preparation (Maestro, 2020). In 1JWH, there are four chains, A, B, C, and D, with solvent and metals; however, we removed Chains B, C, and D for misidentified also removed solvent and metals and kept only Chain A for further studies. While in the case of 1AQ1, chain A and solvent were present; after preparation, we deleted the solvent and kept only chain A. Both proteins

were prepared with the same parameters. The preprocess assigned the bond orders using the CCD database, added hydrogens, created zero-order bonds to metals, created disulphide bonds, filled in missing side chains using Prime, filled in missing loops using Prime, deleted waters beyond 3Å from het groups and generated het states using Epik at pH 7 (Shelley et al., 2007; Jacobson et al., 2004). The structure has refined H-bond assignment with sample water orientations, and to optimise, we used PROPKA at pH 7 and removed the waters beyond hets 3Å. The protein's energy was minimised to obtain the lowest state using the OPLS4 force field (Rostkowski et al., 2011; Lu et al., 2021).

2.2. Ligand preparation and ADMET analysis

DrugBank is an extensive online database with free access to information on medications and drug targets. We downloaded the complete Drug Bank library, imported the data to the workspace, and prepared them to use the LigPrep tool in maestro (Wishart et al., 2018). The maximum number of ligand sizes was kept at 500 atoms, and the OPLS4 forcefield was applied at the ionisation state of Epik, generating possible states at a target pH of 7 and generating the tautomers (Lu et al., 2021). The stereoisomers computations were kept generating at most 32 per ligand and retaining specific chiralities. Further, the QikProp tool was used to calculate the ADMET properties of the ligands kept in check during analysis to pass the ligand that satisfies the criteria (Ioakimidis et al., 2008).

2.3. Molecular docking

Active site prediction was executed using the SiteMap tool to find the best active sites in the selected protein (Maestro. 2020). However, the glide grid generator tool generated the grid for the blind docking approach to get the best pose for the complex (Halgren et al., 2004; Repasky et al., 2007). The screening (Docking) was done under the Virtual Screening Workflow (VSW). In VSW, the prepared library was browsed and checked to run the QikProp to generate the ADMET properties prefiltered by Lipinski's Rule (Ioakimidis et al., 2008; Chen et al., 2020). Epik state penalties were selected in the docking tab and then docked with HTVS, SP, and XP post-process with Prime MMGBSA. Only the top 5% of the HTVS data were used for the SP, and only the top 10% passed to the next phase of XP docking. The binding free energy and surface were calculated for the MMGBSA using 100% of the XP data (Genheden and Ryde, 2015). In order to calculate and sort the data, we also exported the data into CSV format to determine which molecule has the most potential for binding to each of the chosen protein targets. Through the docking approach, we identified Metralindole as a drug candidate against both proteins. Further, after analysing, we merged the protein-ligand to generate the complex for MD simulation.

2.4. Molecular dynamics simulation

Molecular dynamics (MD) is a technique for simulating the physical motions (stability and flexibility) of atoms and molecules, and biologists widely use it to determine any protein or protein-ligand complexity and stability in different solute mediums (Hansson et al., 2002). The MD simulation was performed using the Desmond package, which is thought to be the MD algorithm's fastest and most accurate calculation (Bowers, 2006). The system Builder tool was used to prepare the system in the SPC water model, and the 3D boundary set-up was in an orthorhombic boundary box with a distance of 10Å × 10Å × 10Å in the buffer state. Further, after eliminating the salt and ions placement within 20Å, 6Cl- ion placement is added to neutralise the system for both cases and minimised to build the entire system for MD simulation. Additionally, a simulation production run of 100ns and a recording interval (ps) trajectory of 100 produces 1000 frames at NPT ensemble class. Each complex was maintained at 300K temperature with 1.01325 bar of pressure. Further, the simulation interaction diagram (SID) tool assessed the generated trajectory (Bowers, 2006; Release, 2020).

3. Results and Discussion

3.1. Interaction analysis and ADMET evaluation

For both proteins in complex with the ligand Metralindole, we examined the interaction diagram in 3-D and 2-D to understand if the ligand is fitted in the pocket and shows a proper binding orientation. Each protein's bonding arrangement with the ligand Metralindole is examined separately with the ligand interaction diagram. The Metralindole interacting with the Cyclin-dependent kinase 2 (CDK2) (1AQ1) has shown a Docking score of -5.159 Kcal/mol with MM\GBSA scores of -37.25 and well fitted in the pocket of the protein while interacting with the Pi-cation bond between PHE80 with HN+ atom of the ligand (Figure 1A, B). On the other hand, the compound Metralindole interacting with Casein kinase 2 (CK2) (1JWH) has shown a Docking score of -5.99 Kcal/mol and MM\GBSA scores of -50.09 (Table 1) while interacting with hydrogen bond with LYS68 and O atom and Pi-Pi stacking bond among PHE113 with benzene ring of the ligand (Figure 1C, D). Additionally, Table 1 provides the docking score and information on the various interactions in Kcal/mol. The MM\GBSA score, H-bonding, Vanderwall's forces, molecular weight, and ligand efficiency sa and ligand efficiency in are provided with detailed calculations. Further, along with the standard values of the QikProp tool, the ADMET values are also provided in Table 2 for comparison comprehension. The table also provided the % of oral absorption, the number of rings, Lipinski's rule satisfaction, and many more to understand the compounds' nature in proper directions. All of the results meet the computational requirements and provide evidence that Metralindole can be used to treat Lung Cancer and will not have any significant adverse effects; therefore, experimental validation is necessary before moving forward with human use.

3.2. Molecular dynamics simulation analysis

The molecular dynamics simulation provides an extensive output for deviation of the protein-ligand complex in a defined solute medium and box in neutralised conditions. We kept the job for 100ns in the water using

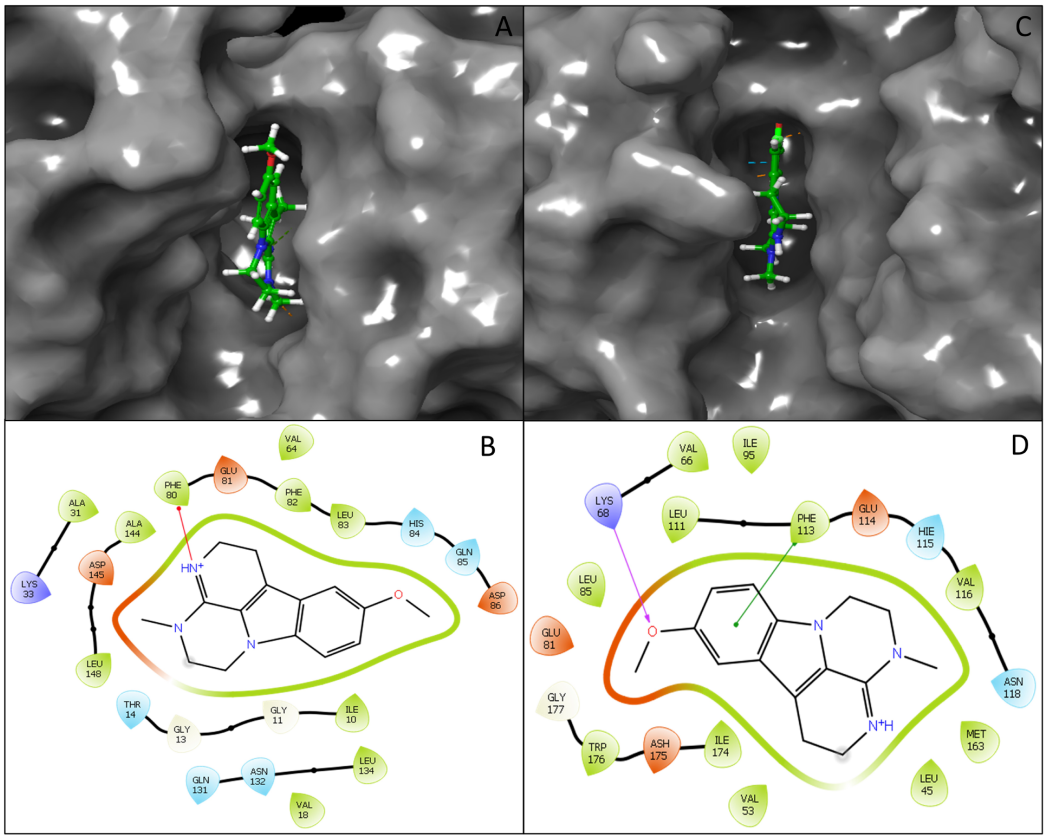

Figure 1. Showing the A) 3-D interaction diagram of 1AQ1 in complex with the Metralindole, B) 2-D interaction of 1AQ1 in complex with the Metralindole, and C) 3-D interaction diagram of 1JWH in complex with Metralindole, D) 2-D diagram of 1JWH in complex with Metralindole.

Table 1. Docking Score and Molecular Mechanics/Generalized Born Surface Area (MMGBSA) Score of Metralindole against both proteins.

PDB ID	Drug Name	Docking Score	MM\GBSA	Prime Hbond	Prime vdW	mol MW	ligand efficiency sa	ligand efficiency ln
1AQ1	Metralindole	-5.159	-37.25	-142.61	-1319.07	255.319	-0.724	-1.308
1JWH	Metralindole	-5.99	-50.09	-175.35	-768.28	255.319	-0.841	-1.519

the SPC model. The detailed analysis of the deviation, fluctuations, and simulation interaction diagram is as follows:

3.2.1. Root-mean-square deviation

The root-mean-square Deviation (RMSD) value is the average change deviation in the protein and ligand in the angstrom (Å) unit with time durations at the nanosecond, which means the RMSD gives proof of consistent performance and the overall stability of the P-L complex. On the left side, Y-axis shows a protein RMSD, and the right Y-axis shows a ligand RMSD. The Cyclin-dependent kinase 2 (CDK2) (1AQ1) complex with Metralindole initially fluctuated at 1.02Å in the protein case while in ligand shows 0.71Å at 0.10 ns, and after that, it continued to perform consistently for the entire simulation duration. At 100ns, the protein shows a deviation of 2.22Å, and the ligand exhibits a deviation of 3.98Å (Figure 2A). The overall deviation for this case can be termed as 1.2 Å for protein, while for the ligand, it was 3.27Å after ignoring the initial deviation. However, the deviation was relatively higher till 10ns, and the complete complex performed steadily. The deviation after ignoring is less than 2Å and can be stated as the deviation for the protein-ligand complex was perfect for biological systems. The case of Casein kinase 2 (CK2) (1JWH) has shown with Metralindole at the initial deviation of 1.40Å in protein, and for the ligand, it shows 2.58Å at0.20 ns, and after performing a complete 100 ns, the protein shows deviation at 2.82Å and for the ligand shows deviation at 4.76Å (Figure 2B). However, for this case, the protein and ligand deviation is less than 2Å after substituting the initial deviation, as it is a common theory that the initial deviation is because of heat and change in the solute medium. The overall performance reveals that the ligand Metralindole has shown better in both instances while staying under less than 2Å after discounting the initial

Table 2. Showing the QikProp values (ADMET) of the ligand Metralindole against the standard values.

Descriptor	QikProp Standard values	Metralindole	Descriptor	QikProp Standard values	Metralindole
#stars	0 – 5	1	QPlogS	−6.5 – 0.5	-4.439
#amine	0 – 1	0	CIQPlogS	−6.5 – 0.5	-4.151
#amidine	0	0	QPlogHERG	concern below −5	-4.305
#acid	0 – 1	0	QPPCaco	<25 poor, >500 great	7447.929
#amide	0 – 1	0	QPlogBB	−3.0 – 1.2	0.387
#rotor	0 – 15	1	QPPMDCK	<25 poor, >500 great	4334.282
#rtvFG	0 – 2	0	QPlogKp	−8.0 – −1.0	-1.219
CNS	−2 (inactive), +2 (active)	1	IP(eV)	7.9 – 10.5	8.097
mol MW	130.0 – 725.0	255.319	EA(eV)	−0.9 – 1.7	0.413
dipole	1.0 – 12.5	2.935	#metab	1 – 8	2
SASA	300.0 – 1000.0	504.626	QPlogKhsa	−1.5 – 1.5	0.467
FOSA	0.0 – 750.0	365.075	HumanOralAbsorption	N/A	3
FISA	7.0 – 330.0	13.062	PercentHumanOralAbsorption	>80% is high, <25% is poor	100
PISA	0.0 – 450.0	126.489	SAfluorine	0.0 – 100.0	0
WPSA	0.0 – 175.0	0	SAamideO	0.0 – 35.0	0
volume	500.0 – 2000.0	858.835	PSA	7.0 – 200.0	25.239
donorHB	0.0 – 6.0	0	#NandO	2 – 15	4
accptHB	2.0 – 20.0	2.25	RuleOfFive	maximum is 4	0
dip^2/V	0.0 – 0.13	0.0100304	RuleOfThree	maximum is 3	0
ACxDN^.5/SA	0.0 – 0.05	0	#ringatoms	N/A	16
glob	0.75 – 0.95	0.8659023	#in34	N/A	0
QPpolrz	13.0 – 70.0	28.782	#in56	N/A	16
QPlogPC16	4.0 – 18.0	7.173	#noncon	N/A	4
QPlogPoct	8.0 – 35.0	10.002	#nonHatm	N/A	19
QPlogPw	4.0 – 45.0	3.878	Jm	N/A	0.562
QPlogPo/w	−2.0 – 6.5	3.86			

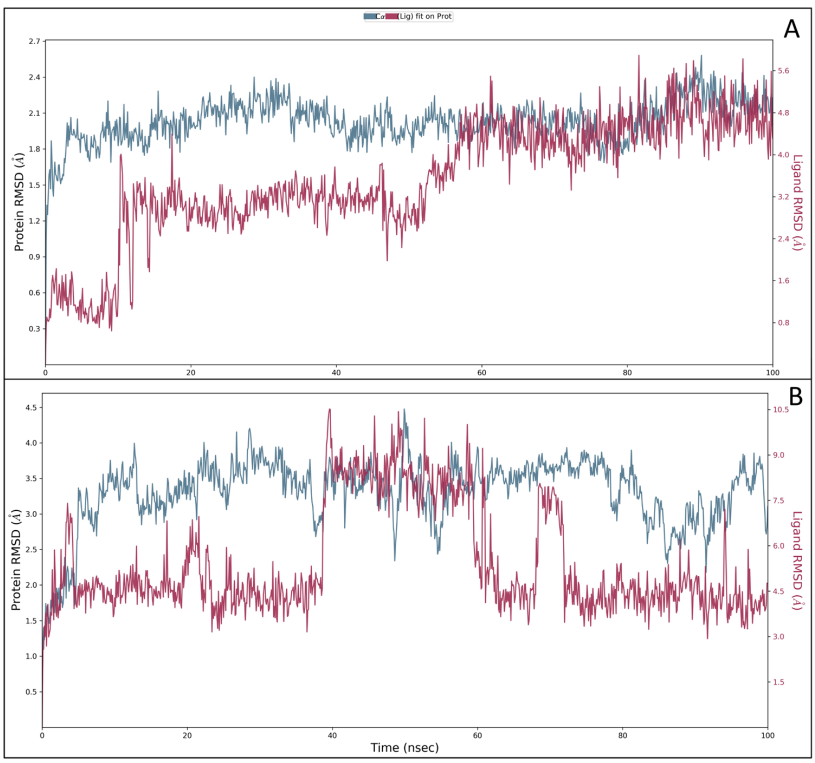

Figure 2. Showing the Root Mean Square Deviation (RMSD) of A) 1AQ1 in complex with the Metralindole and B) 1JWH in complex with the Metralindole.

deviations. The first deviance resulted from the system's direct imposition of a new system. The atoms and residues deviate from the first heating, and the solvation techniques forecast the biased outcomes because of their solubility.

3.2.2. Root-mean-square fluctuation

The root means square fluctuation (RMSF) demonstrates the atomic and residual fluctuations of the ligand and protein. We have examined only the protein fluctuation at the residue level in our investigation regarding residue quantity and interaction with the Metralindole. The residues of Cyclin-dependent kinase 2 (CDK2) (1AQ1) have shown continuously that only some residues have gone beyond the 2Å, which are LEU25, ALA95, SER232, LYS291, PRO292, LEU296, ARG297 (Figure 3A). The Casein kinase 2 (CK2) (1JWH) was also performed solidly during the simulation. The ligand atoms interacting with protein residues are SER2, VAL105, ARG268, and ASP330 (Figure 3B). Nevertheless, the fluctuations among the protein were available for a few residues, and it might be because the protein residues are pretty fluctuating in nature as they have their properties. The protein was stable while resuming the entire RMSF. It displayed several interactions with the ligand Metralindole, supporting the notion that the ligand can obtain and fit and enter the pocket to stop the protein's function and ultimately capture the viral system. Also, the ligand contacted the protein various times during the simulation, shown in green, for proper representation. For both cases, initial residues were highly interactive with the ligand, while the last residues were less interactive during the simulative annealing.

3.2.3. Simulative interaction analysis:

The simulative interaction analysis (SID) has been shown to the ligand-protein contacts during the simulation period, shows the best ligand-protein binding figure, and explains the potent angle of interactions. The Cyclin-dependent kinase 2 (CDK2) (1AQ1) complex with Metralindole has shown a bonding of 2 Pi-cation, one with a benzene ring with LYS89 and another with an NH+ atom with PHE80. Hydrogen bonds interact with NH+ atoms with ASP127, ASP145, ASN132, GLU162, THR14, and GLU12, and hydrogen bonds interact with O atoms with LEU83 and HIS84 (Figure 4A). The Casein kinase 2 (CK2) (1JWH) interaction with ligand, Metralindole has shown that solid interaction with other complexes with 3 Pi-Pi stacking with three benzene rings with HIS160 and hydrogen bonds interactions with NH+ atom among ASP120, LEU45, GLU230, and hydrogen bonds also interact with O atom with ARG47, VAL116, ASP175, LYS68, VAL66, ASN118, GLU81, and ASP120 interacts with a salt bridge (Figure 4B).

Complete simulation analysis shows that NH+ and O atoms form more interactions simultaneously. Ultimate Metralindole fits appropriately in the protein pockets and disrupts the protein's essential functions to stop cancer development. Further, the same protein and ligand interaction during the simulation period were counted and shown in Figure 5. The ligand interaction counts are

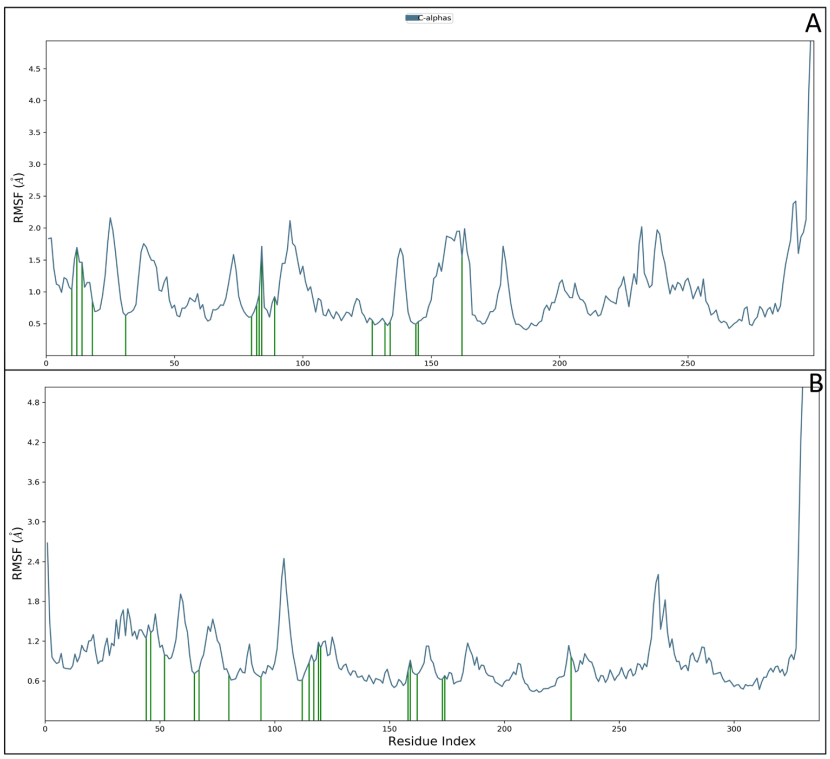

Figure 3. Showing the Root Mean Square Fluctuations (RMSF) of A) 1AQ1 in complex with the Metralindole and B) 1JWH in complex with the Metralindole.

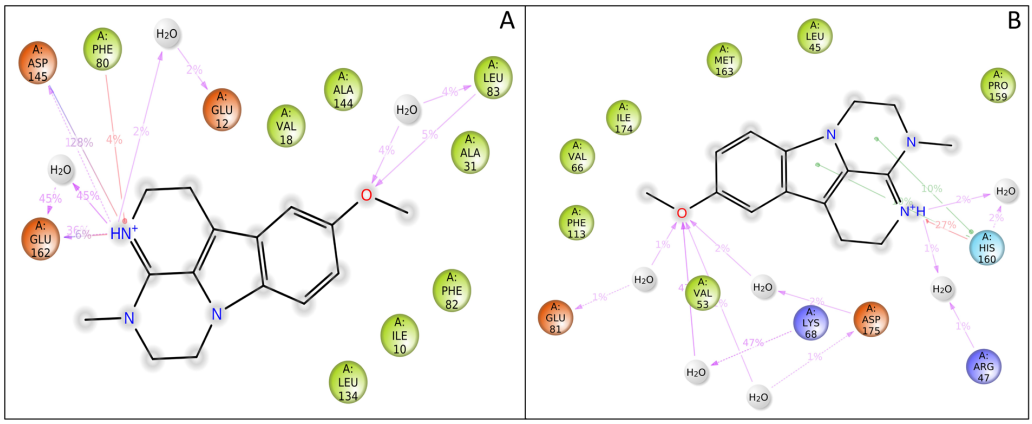

Figure 4. Showing the simulation interaction diagram of A) 1AQ1 in complex with the Metralindole and B) 1JWH in complex with the Metralindole.

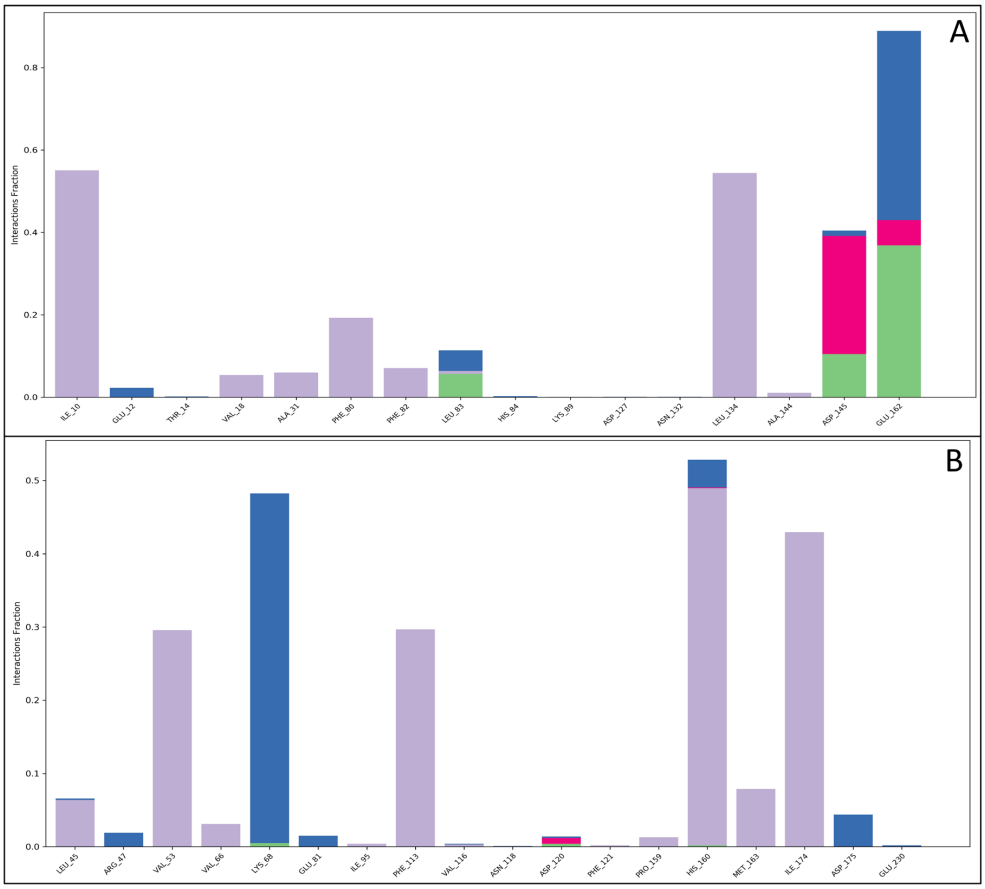

Figure 5. Showing the histogram representation of simulation interaction counts of A) 1AQ1 in complex with the Metralindole and B) 1JWH in complex with the Metralindole.

shown in the histogram, bonding data and a compound's effectiveness with various proteins to clarify the situation further. The overall simulative interaction diagram shows how efficiently the protein and ligands interact with each other and how they have the potential to make a better complex during the natural systems, and it also suggests that the natural system can be seized for cancer development.

4. Conclusions

The CDK2 gene in humans encodes the enzyme cyclin-dependent kinase 2, also known as cell division protein kinase-2. This gene produces a Ser/Thr protein kinase that belongs to the CDK family. It is a catalytic component of the cyclin-dependent kinase complex,

whose activity is confined to the G1-S stage of the cell cycle, during which cells produce the proteins required for mitosis and copy their DNA. A serine-selective protein kinase known as casein kinase-2 has been linked to regulating the circadian rhythm, DNA repair, cell cycle control, and other cellular activities. As a putative defence mechanism for altered cells, CK2 deregulation has been connected to cancer. Since no effective deletion models have been created, proper CK2 function is essential for cell survival. The protein-ligand complex of Metralindole with Cyclin-Dependent Kinase 2 (1AQ1) and Casein kinase 2 (1JWH) are shown a flawless performance during the Docking, MM\GBSA calculations. When we extended the analysis for simulation, the performance was even better, and on the same behalf, it can be concluded that the candidate can be a potential drug compound. However, the drug activity must be validated on cell lines and in-vivo models to properly understand the mechanism of action on lung cancer.

Acknowledgements

The authors would like to thank Imam Abdulrahman Bin Faisal University for supporting the research.

References

AHMAD, S., BANO, N., QAZI, S., YADAV, M.K., AHMAD, N. and RAZA, K., 2022a. Multitargeted molecular dynamic understanding of butoxypheser against SARS-CoV-2: an in silico study. *Natural Product Communications*, vol. 17, no. 7, pp. 1934578X2211154. http://dx.doi.org/10.1177/1934578X221115499.

AHMAD, S., BHANU, P., KUMAR, J., PATHAK, R.K., MALLICK, D., UTTARKAR, A., NIRANJAN, V. and MISHRA, V., 2022b. Molecular dynamics simulation and docking analysis of NF-κB protein binding with sulindac acid. *Bioinformation*, vol. 18, no. 3, pp. 170-179. http://dx.doi.org/10.6026/97320630018170. PMid:36518123.

AHMAD, S., PASHA KM, M., RAZA, K., RAFEEQ, M.M., HABIB, A.H., ESWARAN, M. and YADAV, M.K., 2022c. Reporting dinaciclib and theodrenaline as a multitargeted inhibitor against SARS-CoV-2: an in-silico study. *Journal of Biomolecular Structure & Dynamics*. In press. http://dx.doi.org/10.1080/07391102.2022.2060308. PMid:35451934.

AHMAD, S., CHITKARA, P., KHAN, F.N., KISHAN, A., ALOK, V., RAMLAL, A. and MEHTA, S., 2021. Mobile technology solution for COVID-19: surveillance and prevention. In: K. RAZA, ed. *Computational intelligence methods in COVID-19: surveillance, prevention, prediction and diagnosis.* Singapore: Springer, pp. 79-108. http://dx.doi.org/10.1007/978-981-15-8534-0_5.

ALBERG, A.J., FORD, J.G. and SAMET, J.M., 2007. Epidemiology of lung cancer: ACCP evidence-based clinical practice guidelines. *Chest*, vol. 132, no. 3, pp. 29S-55S. http://dx.doi.org/10.1378/chest.07-1347. PMid:17873159.

ALGHAMDI, Y.S., MASHRAQI, M.M., ALZAMAMI, A., ALTURKI, N.A., AHMAD, S., ALHARTHI, A.A., ALSHAMRANI, S. and ASIRI, S.A., 2022. Unveiling the multitargeted potential of N-(4-Aminobutanoyl)-S-(4-methoxybenzyl)-L-cysteinylglycine (NSL-CG) against SARS CoV-2: a virtual screening and molecular dynamics simulation study. *Journal of Biomolecular Structure & Dynamics*. In press. http://dx.doi.org/10.1080/07391102.2022.2110158. PMid:35971958.

ALTURKI, N.A., MASHRAQI, M.M., ALZAMAMI, A., ALGHAMDI, Y.S., ALHARTHI, A.A., ASIRI, S.A., AHMAD, S. and ALSHAMRANI, S., 2022. In-silico screening and molecular dynamics simulation of drug bank experimental compounds against SARS-CoV-2. *Molecules (Basel, Switzerland)*, vol. 27, no. 14, pp. 4391. http://dx.doi.org/10.3390/molecules27144391. PMid:35889265.

ALZAMAMI, A., ALTURKI, N.A., ALGHAMDI, Y.S., AHMAD, S., ALSHAMRANI, S., ASIRI, S.A. and MASHRAQI, M.M., 2022. Hemi-babim and fenoterol as potential inhibitors of MPro and papain-like protease against SARS-CoV-2: an in-silico study. *Medicina*, vol. 58, no. 4, pp. 515. http://dx.doi.org/10.3390/medicina58040515. PMid:35454354.

BALASUBRAMANIAN, B., AHMAD, S., ALOK, V., KHAN, F.N., ANAND, K., MEHTA, S., EASWARAN, M., MEYYAZHAGAN, A. and SARAVANAN, M., 2021. Exosomes as an emerging nanoplatform for functional therapeutics. In: K. ANAND, M. SARAVANAN, B. CHANDRASEKARAN, S. KANCHI, S. JEEVA PANCHU and Q. CHEN, eds. *Handbook on nanobiomaterials for therapeutics and diagnostic applications.* San Diego: Elsevier, pp. 483-498. http://dx.doi.org/10.1016/B978-0-12-821013-0.00002-7.

BOICE JÚNIOR, J.D., ELLIS, E.D., GOLDEN, A.P., ZABLOTSKA, L.B., MUMMA, M.T. and COHEN, S.S., 2022. Sex-specific lung cancer risk among radiation workers in the million-person study and patients TB-Fluoroscopy. *International Journal of Radiation Biology*, vol. 98, no. 4, pp. 769-780. http://dx.doi.org/10.1080/09553002.2018.1547441. PMid:30614747.

BOWERS, K.J., 2006. Scalable algorithms for molecular dynamics simulations on commodity clusters. In *Proceedings of the 2006 ACM/IEEE Conference on Supercomputing*. New York: IEEE. http://dx.doi.org/10.1109/SC.2006.54.

BOYLE, P. and MAISONNEUVE, P., 1995. Lung cancer and tobacco smoking. *Lung Cancer (Amsterdam, Netherlands)*, vol. 12, no. 3, pp. 167-181. http://dx.doi.org/10.1016/0169-5002(95)00443-5. PMid:7655828.

CHEN, B., HU, B., LI, W. and XUE, J., 2015. Transformation from NSCLC to SCLC: when did it happen? *The Lancet. Oncology*, vol. 16, no. 7, pp. e309. http://dx.doi.org/10.1016/S1470-2045(15)00059-5. PMid:26149876.

CHEN, X., LI, H., TIAN, L., LI, Q., LUO, J. and ZHANG, Y., 2020. Analysis of the physicochemical properties of acaricides based on Lipinski's rule of five. *Journal of Computational Biology*, vol. 27, no. 9, pp. 1397-1406. http://dx.doi.org/10.1089/cmb.2019.0323. PMid:32031890.

FONG, K.M., SRIVASTAVA, S., GOPAL-SRIVASTAVA, R. and KRAMER, B.S., 1999. Molecular genetic basis for early cancer detection and cancer susceptibility. In: S. SRIVASTAVA, D. E. HENSON and A. F. GAZDAR, eds. *Molecular pathology of early cancer*. Amsterdam: IOS Press, pp. 13-26.

GENHEDEN, S. and RYDE, U., 2015. The MM/PBSA and MM/GBSA methods to estimate ligand-binding affinities. *Expert Opinion on Drug Discovery*, vol. 10, no. 5, pp. 449-461. http://dx.doi.org/10.1517/17460441.2015.1032936. PMid:25835573.

HALGREN, T.A., MURPHY, R.B., FRIESNER, R.A., BEARD, H.S., FRYE, L.L., POLLARD, W.T. and BANKS, J.L., 2004. Glide: a new approach for rapid, accurate Docking and scoring. 2. Enrichment factors in database screening. *Journal of Medicinal Chemistry*, vol. 47, no. 7, pp. 1750-1759. http://dx.doi.org/10.1021/jm030644s. PMid:15027866.

HANSSON, T., OOSTENBRINK, C. and VAN GUNSTEREN, W., 2002. Molecular dynamics simulations. *Current Opinion in Structural*

Biology, vol. 12, no. 2, pp. 190-196. http://dx.doi.org/10.1016/S0959-440X(02)00308-1. PMid:11959496.

HOU, J., BHAT, A.M., AHMAD, S., RAZA, K. and QAZI, S., 2022. In silico analysis of ACE2 receptor to find potential herbal drugs in COVID-19 associated neurological dysfunctions. *Natural Product Communications*, vol. 17, no. 8, pp. 1934578X2211185. http://dx.doi.org/10.1177/1934578X221118549.

IOAKIMIDIS, L., THOUKYDIDIS, L., MIRZA, A., NAEEM, S. and REYNISSON, J., 2008. Benchmarking the reliability of QikProp. Correlation between experimental and predicted values. *QSAR & Combinatorial Science*, vol. 27, no. 4, pp. 445-456. http://dx.doi.org/10.1002/qsar.200730051.

JACOBSON, M.P., PINCUS, D.L., RAPP, C.S., DAY, T.J.F., HONIG, B., SHAW, D.E. and FRIESNER, R.A., 2004. A hierarchical approach to all-atom protein loop prediction. *Proteins*, vol. 55, no. 2, pp. 351-367. http://dx.doi.org/10.1002/prot.10613.

KARWASRA, R., AHMAD, S., BANO, N., QAZI, S., RAZA, K., SINGH, S. and VARMA, S., 2022a. Macrophage-targeted punicalagin nanoengineering to alleviate methotrexate-induced neutropenia: a molecular docking, DFT, and MD simulation analysis. *Molecules (Basel, Switzerland)*, vol. 27, no. 18, pp. 6034. http://dx.doi.org/10.3390/molecules27186034. PMid:36144770.

KARWASRA, R., KHANNA, K., SINGH, S., AHMAD, S. and VERMA, S., 2022b. The incipient role of computational intelligence in oncology: drug designing, discovery, and development. In: L. RAZA, ed. *Computational intelligence in oncology*. Singapore: Springer, pp. 369-384. http://dx.doi.org/10.1007/978-981-16-9221-5_21.

KAUL, T., ESWARAN, M., AHMAD, S., THANGARAJ, A., JAIN, R., KAUL, R., RAMAN, N.M. and BHARTI, J., 2020. Probing the effect of a plus 1bp frameshift mutation in protein-DNA interface of domestication gene, NAMB1, in wheat. *Journal of Biomolecular Structure & Dynamics*, vol. 38, no. 12, pp. 3633-3647. http://dx.doi.org/10.1080/07391102.2019.1680435. PMid:31621500.

KHAN, F.N., AHMAD, S. and RAZA, K., 2021a. Clinical applications of next-generation sequence analysis in acute myelogenous leukemia. In: K. RAZA and N. DEY, eds. *Translational bioinformatics applications in healthcare*. Boca Raton: CRC Press. http://dx.doi.org/10.1201/9781003146988-4.

KHAN, F.N., KHANAM, A.A., RAMLAL, A. and AHMAD, S., 2021b. A review on predictive systems and data models for covid-19. In: K. RAZA, ed. *Computational intelligence methods in COVID-19: surveillance, prevention, prediction and diagnosis*, Singapore: Springer, pp. 123-164. http://dx.doi.org/10.1007/978-981-15-8534-0_7.

KHATAMI, M., 2017. *Inflammation, aging and cancer*. Cham: Springer. http://dx.doi.org/10.1007/978-3-319-66475-0.

KHUNTIA, B.K., SHARMA, V., WADHAWAN, M., CHHABRA, V., KIDAMBI, B., RATHORE, S., AGARWAL, A., RAM, A., QAZI, S., AHMAD, S., RAZA, K. and SHARMA, G., 2022. Antiviral potential of Indian medicinal plants against influenza and SARS-CoV: A systematic review. *Natural Product Communications*, vol. 17, no. 3, pp. 1934578X2210869. http://dx.doi.org/10.1177/1934578X221086988.

LAWRIE, A.M., NOBLE, M.E., TUNNAH, P., BROWN, N.R., JOHNSON, L.N. and ENDICOTT, J.A., 1997. Protein kinase inhibition by staurosporine revealed in details of the molecular interaction with CDK2. *Nature Structural Biology*, vol. 4, no. 10, pp. 796-801. http://dx.doi.org/10.1038/nsb1097-796. PMid:9334743.

LU, C., WU, C., GHOREISHI, D., CHEN, W., WANG, L., DAMM, W., ROSS, G.A., DAHLGREN, M.K., RUSSELL, E., VON BARGEN, C.D., ABEL, R., FRIESNER, R.A. and HARDER, E.D., 2021. OPLS4: improving force field accuracy on challenging regimes of chemical space. *Journal of Chemical Theory and Computation*, vol. 17, no. 7, pp. 4291-4300. http://dx.doi.org/10.1021/acs.jctc.1c00302. PMid:34096718.

MAESTRO, S., 2020. *Maestro*. New York: Schrödinger.

NIEFIND, K., GUERRA, B., ERMAKOWA, I. and ISSINGER, O.G., 2001. Crystal structure of human protein kinase CK2: insights into basic properties of the CK2 holoenzyme. *The EMBO Journal*, vol. 20, no. 19, pp. 5320-5331. http://dx.doi.org/10.1093/emboj/20.19.5320. PMid:11574463.

NIMSARKAR, P., GULHANE, P. and SINGH, S., 2022. Understanding the molecular kinetics in NSCLC through computational method. In: S. SINGH, ed. *Systems biomedicine approaches in cancer research*. Singapore: Springer, pp. 129-163. http://dx.doi.org/10.1007/978-981-19-1953-4_7.

RAMLAL, R.A., AHMAD, S., KUMAR, L., KHAN, F.N. and CHONGTHAM, R., 2021. From molecules to patients: the clinical applications of biological databases and electronic health records. In: K. RAZA and N. DEY, eds. *Translational bioinformatics in healthcare and medicine*. London: Academic Press, pp. 107-125. http://dx.doi.org/10.1016/B978-0-323-89824-9.00009-4.

RELEASE, S., 2020. *Maestro-Desmond interoperability tools*. New York: Schrödinger.

REPASKY, M.P., SHELLEY, M. and FRIESNER, R.A., 2007. Flexible ligand docking with Glide. *Current Protocols in Bioinformatics*, vol. 18, no. 1, pp. 12-36. http://dx.doi.org/10.1002/0471250953.bi0812s18.

RIUDAVETS, M., GARCIA DE HERREROS, M., BESSE, B. and MEZQUITA, L., 2022. Radon and lung cancer: current trends and future perspectives. *Cancers (Basel)*, vol. 14, no. 13, pp. 3142. http://dx.doi.org/10.3390/cancers14133142. PMid:35804914.

ROSTKOWSKI, M., OLSSON, M.H., SØNDERGAARD, C.R. and JENSEN, J.H., 2011. Graphical analysis of pH-dependent properties of proteins predicted using PROPKA. *BMC Structural Biology*, vol. 11, no. 1, pp. 6. http://dx.doi.org/10.1186/1472-6807-11-6. PMid:21269479.

SHELLEY, J.C., CHOLLETI, A., FRYE, L.L., GREENWOOD, J.R., TIMLIN, M.R. and UCHIMAYA, M., 2007. Epik: a software program for pK a prediction and protonation state generation for drug-like molecules. *Journal of Computer-Aided Molecular Design*, vol. 21, no. 12, pp. 681-691. http://dx.doi.org/10.1007/s10822-007-9133-z. PMid:17899391.

TARIQUE, M., AHMAD, S., MALIK, A., AHMAD, I., SAEED, M., ALMATROUDI, A., QADAH, T., MURAD, M.A., MASHRAQI, M., ALAM, Q. and AL-SALEH, Y., 2021. Novel severe acute respiratory syndrome coronavirus 2 (SARS-CoV2) and other coronaviruses: a genome-wide comparative annotation and analysis. *Molecular and Cellular Biochemistry*, vol. 476, no. 5, pp. 2203-2217. http://dx.doi.org/10.1007/s11010-020-04027-8. PMid:33564990.

TRIPATHI, M.K., AHMAD, S., TYAGI, R. and DAHIYA, V., 2022. Fundamentals of molecular modeling in drug design. In: M. RUDRAPAL and C. EGBUNA, eds. *Computer Aided Drug Design (CADD): from ligand-based methods to structure-based approaches*. San Diego: Elsevier, pp. 125-155. http://dx.doi.org/10.1016/B978-0-323-90608-1.00001-0.

WARBURG, O., 1956. On the origin of cancer cells. *Science*, vol. 123, no. 3191, pp. 309-314. http://dx.doi.org/10.1126/science.123.3191.309. PMid:13298683.

WISHART, D.S., FEUNANG, Y.D., GUO, A.C., LO, E.J., MARCU, A., GRANT, J.R., SAJED, T., JOHNSON, D., LI, C., SAYEEDA, Z., ASSEMPOUR, N., IYNKKARAN, I., LIU, Y., MACIEJEWSKI, A.,

GALE, N., WILSON, A., CHIN, L., CUMMINGS, R., LE, D., PON, A., KNOX, C. and WILSON, M., 2018. DrugBank 5.0: a major update to the DrugBank database for 2018. *Nucleic Acids Research*, vol. 46, no. D1, pp. D1074-D1082. http://dx.doi.org/10.1093/nar/gkx1037. PMid:29126136.

YADAV, M.K., AHMAD, S., RAZA, K., KUMAR, S., ESWARAN, M., & PASHA KM, M., 2022. Predictive modeling and therapeutic repurposing of natural compounds against the receptor-binding domain of SARS-CoV-2. *Journal of Biomolecular Structure & Dynamics*, vol. 41, no. 5, pp. 1-13.

ZHANG, W., PEI, J. and LAI, L., 2017. Computational multitarget drug design. *Journal of Chemical Information and Modeling*, vol. 57, no. 3, pp. 403-412. http://dx.doi.org/10.1021/acs.jcim.6b00491. PMid:28166637.

ZÜLCH, K.J., 2013. *Brain tumors: their biology and pathology*. Berlin: Springer-Verlag.